
Direct Numerical Simulation of Reacting Turbulent Multi-Species Channel Flow

L. Artal^{1,2} and F. Nicoud²

¹ CERFACS, CFD Team, 42 avenue Gaspard Coriolis, 31057 Toulouse Cedex 1, France

Lea.Artal@cerfacs.fr

² University Montpellier II - CNRS UMR 5149, I3M - CC 51, Place Eugène Bataillon, 34095 Montpellier Cedex 5, France

nicoud@math.univ-montp2.fr

1 Introduction

Rocket engines eject their gases through propulsion nozzles which are subjected to considerable thermal fluxes. However they must stay as light as possible. This requires precise calculations of wall heat flux in order to optimize the design of insulating material. Industrial design codes use Reynolds-Average Navier-Stokes (RANS) methods. High-Reynolds number approaches are often preferred for wall-bounded flows because they require less mesh refinement than their low-Reynolds number counterpart and they are usually more stable. This means using wall functions to assess the momentum/energy fluxes at the solid boundaries knowing the outer flow condition at the first off-wall grid points. The classic logarithmic law is implemented in most of the RANS codes and provides reasonable good results for simple incompressible flows. The trend today is to generalize this wall function to account for more physics [1], [2]. Development of wall functions that take into account strong changes in the density due to strong temperature gradient and fluid non-homogeneity is necessary to simulate parietal heat transfers with a good accuracy and at a moderate cost by using RANS-based design codes. Because the wall heat flux depends on the details of the turbulent flow in the near-wall region, it is essential to analyze detailed relevant data to support the development of such wall models. Classic experimental techniques cannot provide the required space resolution and improved wall functions can hardly be designed or validated due to the lack of relevant data. Direct Numerical Simulations (DNS) can then be used to generate precise and detailed data set of generic turbulent flows [3], [4] under realistic operating conditions. The first objective of this paper is to describe a DNS of anisothermal multi-species channel flow. The second objective is to illustrate how it can be used to improve the existing wall functions and account for more physics in the heat flux assessment.

2 Configuration of the DNS: fluid flow, thermochemistry and solved equations

A sketch of the computational domain and the coordinate system is shown in figure 1.

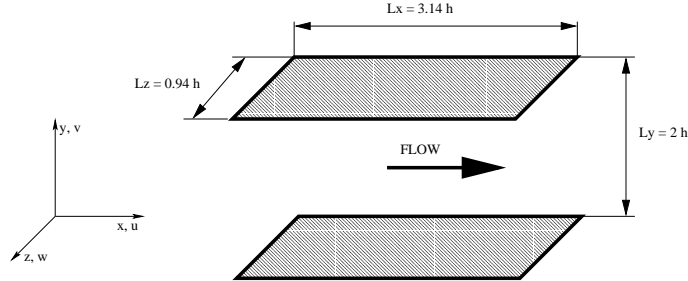


Fig. 1. Geometry of computational domain and coordinate system

A periodic boundary condition is used in the streamwise and spanwise directions, while a non-slip isothermal condition is applied to both walls. In order to save CPU time, the DNS configuration is inspired by the minimal channel flow configuration presented in [5] for instance. The domain dimensions in terms of wall units are $L_x^+ \simeq 560$, $L_y^+ \simeq 360$ and $L_z^+ \simeq 160$ in the streamwise, normal and spanwise directions respectively ($L_i^+ = L_i u_\tau / \nu_w$ where u_τ denotes the friction velocity and ν_w the kinematic viscosity at the wall). The mesh contains $17 \times 130 \times 33$ nodes. The associated resolution in x and z which is $\Delta x^+ \simeq 35$ and $\Delta z^+ \simeq 5$, allows to capture the elongated turbulence structure. Uniform in the streamwise and spanwise directions, the grid spacing of the parallelepipedic mesh is refined with a hyperbolic tangent law in the direction normal to the flow, in order to be able to solve the viscous sub-layer. This results in $\Delta y^+ \simeq 0.9$ at the wall and $\Delta y^+ \simeq 5$ near the centerline.

The Mach number Ma is about 0.2 so that the effects of compressibility can be neglected and the CFL condition is not too restrictive. For the friction Reynolds number Re_τ , the classic value 180 encountered in the literature of turbulent channels with inert walls ([6] for instance) is chosen. Table 1 gathers a few data representative of the flow configuration.

P (MPa)	T_{wall} (K)	T_{mean} (K)	h (mm)	Ma_{max}	$Re_\tau = \mathbf{u}_\tau h / \nu_w$	$Re = U_{\text{max}} h \bar{\rho} / \bar{\mu}$
10	2700	3000	0.115	0.2	180	3400

Table 1. Data related to the DNS configuration

This computation is initialized thanks to an already turbulent solution coming from a DNS performed on the same configuration but without chemistry, and

having reached a converged state.

The ejected gases from propulsion nozzles form a reactive³ mixture made up with about a hundred gaseous species. The DNS is performed with a gaseous mixture representative of these gases. The transport properties of this equivalent mixture are obtained thanks to the EGLIB library [7]. The DNS is realized with a Schmidt number per species indicated in table 2, and a Prandtl number for the mixture equal to 0.47. Because the numerical code used does not assume chemical equilibrium, a kinetic scheme which reproduces concentration changes in the equivalent mixture through seven chemical reactions has been tuned, thanks to the GRI-Mech data [8]. In report [9], it has been verified that this kinetic scheme gives the right compositions at equilibrium.

Species	H ₂	N ₂	CO	H ₂ O	H	CO ₂	OH
Sc	0.20	0.87	0.86	0.65	0.15	0.98	0.53

Table 2. Schmidt number Sc of each gaseous species at $P = 10$ MPa

We consider the three-dimensional compressible unsteady Navier-Stokes equations with chemistry and spatially constant source terms. Because of periodicity in the streamwise direction, a source term S_{qdm} that acts like a pressure gradient must be added to the streamwise component of the momentum conservation equation. Moreover, it is necessary to add a volumic source term S_e to the total energy conservation equation in order to compensate for the thermal losses occurring at the isothermal wall. This volumic source term is constant in space so that it does not modify the temperature profile and drive the averaged temperature in the channel towards the target value T_{mean} . T_{mean} is fixed so that the temperature gradient in the boundary layer of a propulsion nozzle is reproduced. The computation is performed with the AVBP parallel code developed at CERFACS and dedicated to DNS/LES of reacting flows on unstructured and hybrid meshes. This code has been thoroughly validated [10].

3 Results of the DNS: chemical equilibrium, shear stress and heat flux

Because of very high pressure/temperature values and extreme thinness of boundary layer, no detailed experimental data are available for typical flows in nozzles of rocket motors, and virtually no model exists for the assessment of the corresponding wall fluxes. Consistently, the present DNS results are

³ In addition, they chemically react with the carbon-coated walls of the nozzles through an ablation reaction. However, this topic will not be dealt with in this paper.

analyzed in terms of wall function: the ability of existing laws-of-the-wall to reproduce the results is first tested; then, these laws-of-the-wall are enriched thanks to the data generated by the DNS.

Knowing the mean temperature profile, the profiles of mass fractions at equilibrium can be obtained thanks to the equilibrium curves of the equivalent mixture and compared to the profiles obtained by post-processing the fields of mass fractions from the DNS. Such a comparison is made in figure 2 which shows that the hypothesis of chemical equilibrium is valid in the DNS. In terms of wall function, it means that a law for temperature and velocity is enough to determine the wall heat flux and the shear stress.

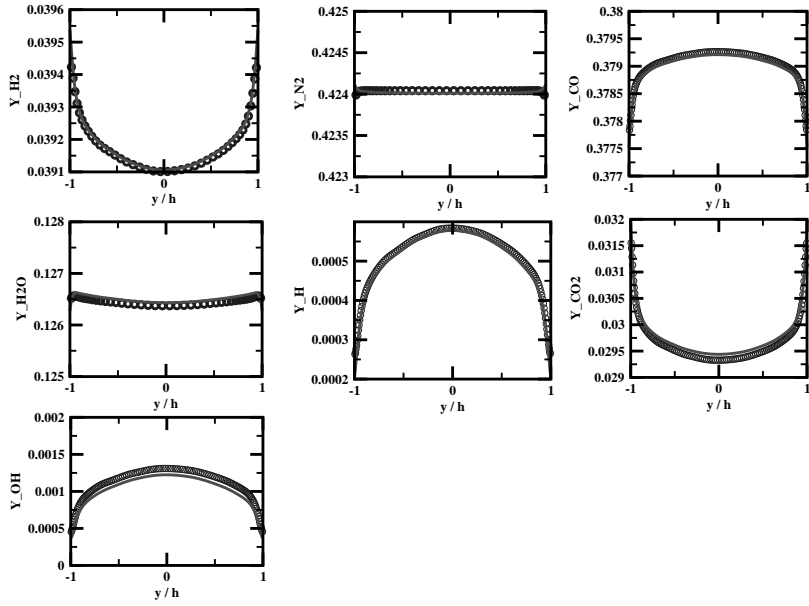


Fig. 2. Chemical equilibrium - Symbols: Mean mass fractions from the DNS; Continuous line: Mass fractions at equilibrium from the DNS temperature profile

The derivation of logarithmic wall functions usually relies on the existence of a zone with constant friction/heat flux. For the shear stress and the heat flux in the turbulent wall region, such an assumption leads to:

$$\tau_w = -\bar{\rho} \overline{u'v'} \approx \mu_t \frac{d\bar{u}}{dy} \quad (1)$$

when the Boussinesq hypothesis is applied, and to:

$$q_w = \bar{\rho} \bar{C}_p \overline{v'T'} \approx -\frac{\mu_t C_p}{Pr_t} \frac{\partial \bar{T}}{\partial y} \quad (2)$$

When chemical composition evolves, the mixture features change, a heat flux related to species diffusion exists and the energy equation admits a chemical source term.

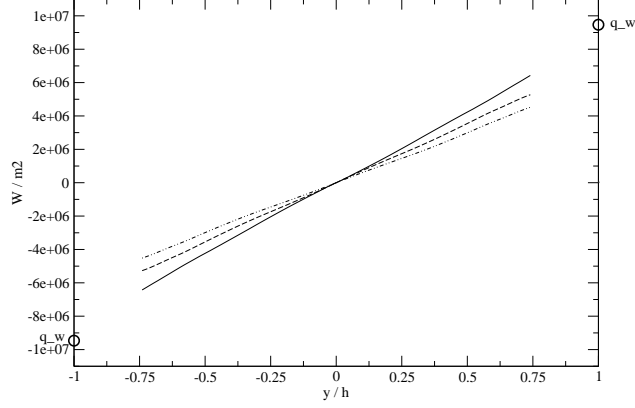


Fig. 3. Heat flux in the turbulent zone - Continuous line: Total heat flux; Dashed line: Sum of the turbulent heat flux and of the turbulent species diffusion term; Dashes and points: Turbulent heat flux

Figure 3 points out that in the turbulent zone the total heat flux can be reasonably approximated by the sum of the turbulent heat flux $\bar{\rho} \bar{C}_p \overline{v'T'}$ and of the turbulent species diffusion term $\sum_{k=1}^{n.s} \bar{\rho} \overline{v'Y'_k} \Delta h_{f,k}^0$. The wall heat flux can then be obtained by extrapolating the curves up to the wall. Because of the low Reynolds number of this DNS, the Fourier term and the turbulent species diffusion term are found to be of the same order of magnitude in the turbulent zone. This explains the discrepancy noticed between the total heat flux and its approximation. However, we anticipate the Fourier term to become truly negligible when the turbulent Reynolds number is large enough. Therefore, at high Reynolds number, and when there is no forcing term, the wall turbulent zone should be characterized by:

$$\bar{\rho} \bar{C}_p \overline{v'T'} + \sum_{k=1}^{n.s} \bar{\rho} \overline{v'Y'_k} \Delta h_{f,k}^0 \approx q_w \quad (3)$$

which differs from equation (2).

The classic logarithmic law does not represent the present results, as shown in figure 4 which compares the non-dimensional temperature profile T^+ given by various laws (the logarithmic law, the Kader correlation [11] and the new wall function proposed in this paper) to the one coming from DNS. T^+ is defined by $T^+ = (T_w - T)/T_\tau$, where $T_\tau = q_w/(\rho_w C_p u_\tau)$ denotes the friction temperature, q_w the wall heat flux and C_p the mixture mass heat capacity at constant pressure.

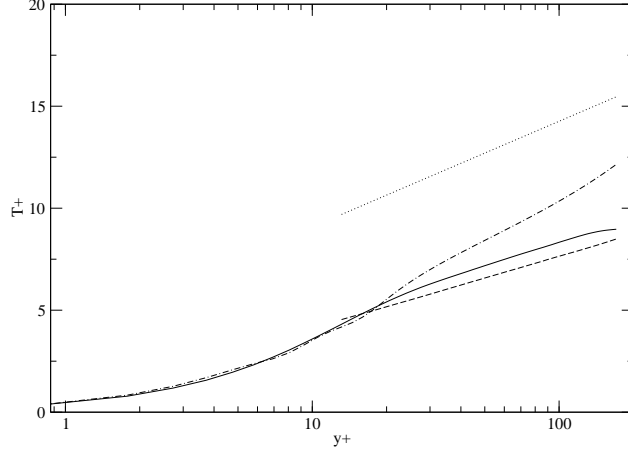


Fig. 4. T^+ profiles - Continuous line: DNS results; Dashed line: New wall function; Dashes and points: Kader correlation; Points: Logarithmic law $T^+ = (0.9/2.5)\ln y^+ + 3.9$

Two main reasons have been identified for this disagreement: a) on the contrary to the Kader correlation, the log law does not account for variations in the molecular Prandtl number and is made for cases with molecular Prandtl number close to unity (it is 0.47 in the present study), b) even if the mixture is always close to chemical equilibrium, the heat release due to chemical reactions is sufficiently large and non uniform over space to prevent the classic constant turbulent heat flux assumption from holding and equation (3) should be used instead of (2). Although in better agreement with the DNS data than the logarithmic law, the Kader correlation does not reflect DNS because of chemistry influence.

In order to account for the chemistry effects in the wall region description, a new wall function is derived from equation (3).

The turbulent heat flux is again modeled by the classic formula:

$$\bar{\rho} \bar{C}_p \overline{v'T'} \approx -\frac{\mu_t C_p}{Pr_t} \frac{\partial \bar{T}}{\partial y} \quad (4)$$

The turbulent species diffusion terms must be modeled too. For each species, one makes use of the following approximation, valid under the chemical equilibrium assumption:

$$\bar{\rho} \overline{v'Y'_k} \approx -\frac{\mu_t}{Sc_{k,t}} \frac{W_k}{\bar{W}} \frac{\partial \bar{X}_k}{\partial y} \approx -\frac{\mu_t}{Sc_{k,t}} \frac{W_k}{\bar{W}} \frac{d\bar{X}_k}{d\bar{T}} \frac{\partial \bar{T}}{\partial y} \quad (5)$$

Writing equation (1) in terms of non-dimensional variables and integrating it, the following logarithmic approximation is found for the Van Driest transformation [12], [13]:

$$u_{VD}^+ = \int_0^{U^+} \sqrt{\frac{\bar{\rho}}{\rho_w}} du^+ = \frac{1}{\kappa} \ln y^+ + C \quad (6)$$

Dividing equation (3) by equation (1) and injecting equations (4) and (5) yield:

$$\frac{T}{T_w} = C_1 - \alpha U^+ \quad (7)$$

with

$$\alpha = \frac{C_p B_q}{\frac{C_p}{Pr_t} + \frac{1}{W} \sum_{k=1}^{ns} \frac{1}{Sc_{k,t}} W_k \frac{dX_k}{dT} \Delta h_{f,k}^0} \quad (8)$$

and

$$B_q = \frac{q_w}{\rho_w C_p u_\tau T_w} = -\frac{T_\tau}{T_w} \quad (9)$$

Assuming that the thermodynamic pressure is constant through the boundary layer, combination of equations (6) and (7) leads to the following coupled wall function including chemistry and sensitivity to the molecular Prandtl number:

$$\begin{cases} \frac{2}{\alpha} \left(\sqrt{C_1} - \sqrt{C_1 - \alpha U^+} \right) = \frac{1}{\kappa} \ln y^+ + C \\ T^+ = \frac{T - T_w}{T_\tau} = \frac{\alpha}{B_q} U^+ + K(Pr) \end{cases} \quad (10)$$

At this point, we still have the liberty to fix the constant of integration C_1 . To do so, we impose the wall function (10) to be coherent with the Kader correlation in the limit case of a passive scalar. This implies $C_1 = 1 - B_q K(Pr)$, with $K(Pr) = \beta(Pr) - Pr_t C + (2.12 - (Pr_t/\kappa)) \ln(100)$ and $\beta(Pr) = (3.85 Pr^{1/3} - 1.3)^2 + 2.12 \ln(Pr)$ when we impose our wall function to give the same T^+ as the Kader correlation at $y^+ = 100$. Note that this definition makes C_1 close to unity, which is consistent with the experimental data [14].

4 Conclusion

The DNS of reacting turbulent multi-species wall-bounded flow presented in this paper provided accurate data, which highlighted the chemistry influence on the heat flux and the known sensitivity of the heat flux to the molecular Prandtl number. Thanks to these results, a new wall function which takes into account chemistry and molecular Prandtl number was derived and successfully a priori tested.

5 Acknowledgements

The authors are grateful to Snecma Propulsion Solide (Groupe SAFRAN) for supporting this work, and to the CINES (Centre Informatique National pour l'Enseignement Supérieur) for the access to supercomputer facilities.

References

1. T. J. Craft, A. V. Gerasimov, H. Iacovides, and B. E. Launder. Progress in the generalization of wall-function treatments. *International Journal of Heat and Fluid Flow*, pages 148–160, 2002.
2. R. H. Nichols and C. C. Nelson. Wall function boundary conditions including heat transfer and compressibility. *AIAA Journal*, 42(6):1107–1114, June 2004.
3. P. Moin and K. Mahesh. DIRECT NUMERICAL SIMULATION: A Tool in Turbulence Research. *Annual Review of Fluid Mechanics*, pages 539–578, 1998.
4. N. Kasagi and O. Iida. Progress in direct numerical simulation of turbulent heat transfer. *Proceedings of the 5th ASME/JSME Joint Thermal Engineering Conference*, March 15-19 1999.
5. J. Jiménez and P. Moin. The minimal flow unit in near-wall turbulence. *Journal of Fluid Mechanics*, 225:213–240, 1991.
6. J. Kim, P. Moin, and R. Moser. Turbulence statistics in fully developed channel flow at low Reynolds number. *Journal of Fluid Mechanics*, 177:133–166, 1987.
7. A. Ern and V. Giovangigli. *EGLIB: A General-purpose FORTRAN Library For Multicomponent Transport Property Evaluation*. CERMICS and CMAP, 2001.
8. http://www.me.berkeley.edu/gri_mech.
9. L. Artal. Modélisation des flux de chaleur stationnaires pour un mélange multi-espèce avec transfert de masse à la paroi, Rapport d'avancement Année 2. Technical Report CR/CFD/04/113, SNECMA-CERFACS-UMII, 2004.
10. http://www.cerfacs.fr/cfd/avbp_code.php.
11. B. A. Kader. Temperature and Concentration Profiles In Fully Turbulent Boundary Layers. *International Journal of Heat and Mass Transfer*, 24(9):1541–1544, 1981.
12. E. R. Van Driest. Turbulent boundary layers in compressible fluids. *J. Aero. Sci.*, 18(3):145–160, 1951.
13. P. G. Huang and G. N. Coleman. Van Driest transformation and compressible wall-bounded flows. *AIAA Journal*, 32(10), 1994.
14. P. Bradshaw. Compressible turbulent shear layers. *Ann. Rev. Fluid Mech.*, 9:33–54, 1977.